Biochemical Pharmacology 80 (2010) 1690–1699

Contents lists available at ScienceDirect

Biochemical Pharmacology

journal homepage: www.elsevier.com/locate/biochempharm

Prevention of *in vitro* hepatic stellate cells activation by the adenosine derivative compound IFC305

Gabriela Velasco-Loyden [a], Julio Isael Pérez-Carreón [b], José Fernando Cabello Agüero [a], Pilar Cabrales Romero [a], Susana Vidrio-Gómez [a], Lidia Martínez-Pérez [a], Lucia Yáñez-Maldonado [a], Rolando Hernández-Muñoz [a], Marina Macías-Silva [a], Victoria Chagoya de Sánchez [a,*]

[a] Departamento de Biología Celular y Desarrollo, Instituto de Fisiología Celular, Universidad Nacional Autónoma de México (UNAM), México 04510, D.F., Apdo. postal 70-243, Mexico
[b] Instituto Nacional de Medicina Genómica (INMEGEN), Periférico sur 4214, México D.F., 01900, Mexico

ARTICLE INFO

Article history:
Received 3 July 2010
Accepted 23 August 2010

Keywords:
Liver
Fibrosis
Hepatic stellate cells
Adenosine
Cell proliferation
Cell differentiation

ABSTRACT

We have previously shown that adenosine and the aspartate salt of adenosine (IFC305) reverse pre-established CCl_4-induced cirrhosis in rats. However, their molecular mechanism of action is not clearly understood. Hepatic stellate cells (HSC) play a pivotal role in liver fibrogenesis leading to cirrhosis, mainly through their activation, changing from a quiescent adipogenic state to a proliferative myofibrogenic condition. Therefore, we decided to investigate the effect of IFC305 on primary cultured rat HSC. Our results reveal that this compound suppressed the activation of HSC, as demonstrated by the maintenance of a quiescent cell morphology, including lipid droplets content, inhibition of α-smooth muscle actin (α-SMA) and collagen α1(I) expression, and up-regulation of MMP-13, Smad7, and PPARγ expression, three key antifibrogenic genes. Furthermore, IFC305 was able to repress the platelet-derived growth factor (PDGF)-induced proliferation of HSC. This inhibition was independent of adenosine receptors stimulation; instead, IFC305 was incorporated into cells by adenosine transporters and converted to AMP by adenosine kinase. On the other hand, addition of pyrimidine ribonucleoside as uridine reversed the suppressive effect of IFC305 on the proliferation and activation of HSC, suggesting that intracellular pyrimidine starvation would be involved in the molecular mechanism of action of IFC305. In conclusion, IFC305 inhibits HSC activation and maintains their quiescence *in vitro*; these results could explain in part the antifibrotic liver beneficial effect previously described for this compound on the animal model.

1. Introduction

Liver fibrosis is a wound-healing process in response to a chronic liver injury. Fibrosis is characterized by an increased accumulation of extracellular matrix (ECM) proteins, especially type I collagen. Hepatic stellate cells (HSC) are the main ECM producing cells in the fibrotic liver. In normal liver, HSC are quiescent vitamin A-storing cells, however, after a fibrogenic stimulus, HSC are activated and transdifferentiated to myofibroblast-like cells, with a phenotype characterized by loss of vitamin A storage, increased proliferation, expression of α-SMA, and excessive synthesis of ECM proteins [1]. Although the molecular mechanism for the HSC activation is not completely understood, it is well accepted that suppression of HSC activation and proliferation are important therapeutic strategies for the prevention or treatment of liver fibrosis.

Adenosine is a natural purine ribonucleoside present within and outside cells with many physiological actions. Adenosine is mainly formed by the phosphohydrolysis of adenine nucleotides and by hydrolysis of S-adenosyl homocysteine formed by the demethylation of S-adenosyl methionine. Extracellular adenosine can exert its function through activation of adenosine receptors or can be transported into the cells via nucleoside transporters. Within the cell, adenosine is phosphorylated to AMP by adenosine kinase, deaminated to inosine by adenosine deaminase or converted to S-adenosyl-homocysteine by S-adenosylhomocysteine hydrolase [2,3]. Accumulation of intracellular AMP can allostericaly stimulates AMP-activated protein kinase activity (AMPK) [4] or can reduce pyrimidine nucleotides, by a process known as "pyrimidine starvation" [5–7]. Adenosine has been described by our group as an important compound that prevents and reverses cirrhosis induced by carbon tetrachloride (CCl_4) in rats [8–13]. We have determined that adenosine reverses

Abbreviations: HSC, hepatic stellate cells; IFC305, aspartate salt of adenosine; CCl_4, carbon tetrachloride; α-SMA, α-smooth muscle actin; MMP, matrix metalloproteinase; PPARγ, peroxisome proliferator-activated receptor gamma; PDGF, platelet-derived growth factor; ERK, extracellular regulated kinase; p70S6K, p70S6 kinase; JNK, c-Jun N-terminal kinase; TIMP, tissue inhibitor of metalloproteinases; TGF-β, transforming growth factor-β; AMPK, AMP-activated protein kinase.

* Corresponding author. Tel.: +52 5 556225614; fax: +52 5 556225611.
E-mail address: vchagoya@ifc.unam.mx (V.C. de Sánchez).

0006-2952/$ – see front matter © 2010 Elsevier Inc. All rights reserved.
doi:10.1016/j.bcp.2010.08.017

experimental cirrhosis by enhancing liver collagenolytic activity, stimulating hepatocyte proliferative capacities, as well as accelerating normalization of parameters indicative of liver function and reducing levels of oxidative stress. Adenosine's beneficial effects have been associated with a cell redox state modulation, maintenance of liver energy availability, and an adequate mitochondrial function of hepatic cells [8–13]. Recently, we synthesized the aspartate salt of adenosine IFC305, which has a longer half-life in the liver and its beneficial effects on CCl_4-induced cirrhosis in rats are achieved with a lower dose [14]. IFC305 functions include the hepatoprotective effect of adenosine and the additional possible effect of aspartate favoring the urea cycle [15]. IFC305 reverses hepatic fibrosis decreasing expression of some fibrogenic genes like collagen α1(I) and Tgfb1 and reducing activated HSC in CCl_4-treated rats [14]. Although the capacity of IFC305 to reverse fibrosis has been characterized in liver rats, the study of the effect of this compound on individual cells involved in hepatic fibrogenesis, such as HSC, would clarify the mechanism of action at the molecular level. In the present study, we focused on the effect of IFC305 on HSC. Herein, we report that IFC305 inhibits the activation of HSC cultivated *in vitro*, and we explore the possible mechanism of action.

2. Materials and methods

2.1. Chemicals

8-Cyclopentyl-1,3-dipropylxanthine (DPCPX, A_1 antagonist), MSX-3 (A_{2A} antagonist), MRS 1754 (A_{2B} antagonist), MRS 1523 (A_3 antagonist), S-(4-nitrobenzyl)-6-thioinosine (NBTI, adenosine transporter inhibitor), dipyridamole (adenosine transporter inhibitor), 5′-amino-5′-deoxyadenosine p-toluenesulfonate salt (AMDA, adenosine kinase inhibitor), salts and detergents were from Sigma–Aldrich (St. Louis, MO). Human PDGF-BB and erythro-9-(2-hydroxy-3-nonyl) adenosine hydrochloride (EHNA, adenosine deaminase inhibitor) were from Calbiochem (La Jolla, CA). Pronase was from Roche Diagnostics (Indianapolis, IN). Collagenase Type 4 was from Worthington Biochemical Corporation (Lakewood, NJ). IFC305 is the aspartate salt of adenosine synthesized by Probiomed S.A. de C.V. (http://www.probiomed.com.mx, Mexico City, Mexico).

2.2. Hepatic stellate cell isolation and culture

HSC were isolated from normal male Wistar rats (500–600 g body weight) by *in situ* enzymatic digestion of the liver with collagenase/pronase and density gradient ultracentrifugation with Accudenz® (Accurate Chemical, Westbury, NY) as previously described [16]. HSC were cultured on plastic dishes in DMEM (Invitrogen, Carlsbad, CA) containing 10% fetal bovine serum (FBS) (Multicell Wisent Inc., La Jolla, CA), 100 U/ml penicillin, and 100 μg/ml streptomycin (DMEM-10% FBS). The cells were seeded at a density of 2.5×10^6 (7 days of culture) or 5×10^6 (2 days of culture) per culture dish (diameter 10 cm). After 24 h of isolation, the culture medium was replaced with DMEM-10% FBS containing the indicated concentration of IFC305. The medium was changed every other day for a total of 7 days, for continuous treatment or for only 24 h, as indicated. Cell death was measured with an ELISA kit (Cell Death Detection ELISA plus; Roche Diagnostics, Indianapolis, IN) and lactate dehydrogenase release was measured with In Vitro Toxicology Assay Kit, Lactic Dehydrogenase based (Sigma–Aldrich, St. Louis, MO), according to manufacturer's instructions.

2.3. Staining of lipids with Oil Red O

HSC were cultured on glass slides, fixed in 10% formalin saline for 5 min, washed with water and then placed in absolute propylene glycol for 5 min. Cells were stained during 15 min with a solution of 0.5% Oil Red O dissolved in propylene glycol pre-warmed at 60 °C, rinsed in 85% propylene glycol for 5 min. After rinsing with distilled water, cells were counterstained with Mayers hematoxylin, neutralized in 10% ammonia, and mounted with aqueous mounting medium.

2.4. Immunofluorescence staining

HSC were cultured on glass slides, fixed in 4% paraformaldehyde in PBS for 30 min at 4 °C and permeabilized with 0.1% Triton X-100 in PBS for 3 min at room temperature. Unspecific binding sites were blocked with 1% bovine serum albumin (BSA) in PBS for 20 min. F-actin stress fibers were stained incubating the cells with Alexa Fluor 532 phalloidin (Invitrogen, Carlsbad, CA) in PBS with 1% BSA for 20 min. Finally, cells were mounted on Vectashield mounting medium (Vector Laboratories, Burlingame, CA). Fluorescence was visualized with an Olympus Inverted Microscope model IX71 and images captured with Evolution/QImaging Digital Camera (Media Cybernetics, Bethesda, MD).

2.5. Real-time quantitative polymerase chain reaction (qPCR)

Total RNA from HSC was isolated using RNeasy Mini Kit (Qiagen, Inc., Valencia, CA). For cDNA synthesis, reverse transcription was performed using the High-Capacity cDNA Archive Kit (Applied Biosystems, Foster City, CA) following the manufacturer's protocol. Real-time quantitative PCR reactions (qPCR) were done in the ABI PRISM 7000 Sequence Detection System (Applied Biosystems Foster City, CA) using Platinum SYBR Green qPCR SuperMix-UDG with ROX Kit (Invitrogen, Carlsbad, CA) according to manufacturer's instructions. The primers used were: Collagen α(1)I, forward 5′-TGGATTCCCGTTCGAGTACG-3′ and reverse 5′-AGGTGATGTTCTGGGAGGCC-3′; MMP-13, forward 5′-AAAGACTATCCCCGCCTCAT-3′ and reverse 5′-TGGGCCCATTGAAAAAGTAG-3; TIMP-1, forward 5′-GCCGTTTAAGGAACGGAAAT-3′ and reverse 5′-ATGGCTGAACAGGGAAACAC-3′; Smad7, forward 5′-GCATCTTCTGTCCCTGCTTC-3′ and reverse 5′-CCGGTCTTCCTTTCCTTTTC-3; PPARγ, forward 5′-GACATCCCGTTCACAAGAGC-3′ and reverse 5′-GCTTTATCCCCACAGACTCG-3′; ARP, forward 5′-AGGTGGTGCTGATGGGCA-3′ and reverse 5′-CCTCCGGATGTGAGGCAG-3′. Relative mRNA transcript levels were expressed in arbitrary units as n-folds of untreated control (mean ± SEM) after normalization to the acidic ribosomal protein (ARP) mRNA.

2.6. Western blotting

Cultured HSC were washed twice with phosphate-buffered saline (PBS), and were lysed with cell lysis buffer (50 mM Tris, pH 7.4, 150 mM NaCl, 0.5% Triton X-100, containing a mixture of protease and phosphatase inhibitors). Lysates were centrifuged and the supernatant was used as whole cell protein. Cell lysates (20 μg protein/well) were electrophoresed in SDS-polyacrylamide gels and transferred to PDVF membranes. Membranes were blocked for 1 h with 5% nonfat dry milk in TBST (50 mM Tris, 150 mM NaCl at pH 7.4, and 0.05% Tween 20). Protein was detected by incubating overnight at 4 °C with antibodies against α-SMA (Sigma–Aldrich, St. Louis, MO), cyclin D1, cyclin E, p27 (kip1), β-actin, phospho-AKT (Ser-473) (Santa Cruz Biotechnology, Santa Cruz, CA), phospho-p44/42 Map kinase (Thr-202/Tyr-204), phospho-p70S6K (Thr-421/Ser-424), phospho-SAPK/JNK (Thr-183/Tyr-185), SAPK/JNK, and phospho-AMPK (Thr-172) (Cell Signaling Technology, Danvers, MA). Primary antibody binding was detected with the respective horseradish peroxidase-conjugated secondary antibody using Western blotting luminol reagent (Santa Cruz Biotechnology, Santa Cruz, CA).

2.7. Pull-down assay of GTP-bound Rho

Rho activation was analyzed with the Rho activation assay kit (Upstate, Temecula, CA) following manufacturer's instructions. Briefly, cultured HSC were washed twice with Tris-buffered saline (TBS) and lysed with Mg^{2+} lysis/wash buffer (MLB) containing a mixture of protease and phosphatase inhibitors. The extracts were incubated for 45 min with the Rho Assay Reagent (Rhotekin RBD bound to glutathione-agarose beads). Agarose beads were washed three times with MLB and bound proteins were eluted in Laemmli reducing sample buffer and analyzed by Western blotting with anti-Rho (-A, -B, -C) clone 55. An aliquot from each extract without agarose beads was also analyzed and corresponds to total Rho.

2.8. Cell proliferation assay

Cell proliferation was assessed by BrdU incorporation using a colorimetric BrdU cell proliferation enzyme linked immunoassay kit (ELISA) (Roche Diagnostics Co., Indianapolis, IN). Freshly isolated HSC were seeded at a density of 2×10^4 cells/well in a 96-well plate, incubated overnight with DMEM-10% FBS, and serum starved for 24 h. Then the cells were stimulated with PDGF-BB (20 ng/ml) in the presence of the indicated concentration of IFC305 in DMEM with BrdU for 24 h. In some experiments the indicated inhibitors or uridine were added 30 min before IFC305 and PDGF-BB addition. After 24 h, BrdU incorporation in the proliferating cells was detected following manufacturer's instructions.

2.9. Statistical analysis

All values were expressed as mean ± SEM of three independent experiments. Statistical analysis was performed using the unpaired, non-parametric Student's *t*-test. Differences with a *p*-value of less than 0.05 were considered statistically significant.

3. Results

3.1. IFC305 prevents the activation of HSC in vitro

Freshly isolated HSC cultured on plastic become spontaneously activated and transdifferentiate from a quiescent to a myofibroblast phenotype, similarly to the activation process seen *in vivo* [1]. HSC activation is accompanied by changes in cell morphology; after 7 days of culture, HSC displayed a myofibroblast morphology, characterized by expanded and flatten shape, loss of refringent vesicles and extensive F-actin stress fibers (Fig. 1B, E and H). In contrast, HSC cultured in the presence of IFC305 (2.5–5 mM) maintained a stellate cell-like morphology with dendrite-like processes, abundant perinuclear lipid droplets and reduced F-actin stress fibers (Fig. 1C, F and I), similarly to quiescent freshly isolated cells (Fig. 1A, D and G). Lactate dehydrogenase release and trypan blue assays, as well as apoptosis detection revealed that there were neither cytotoxic effects nor differences in cell viability in the presence of IFC305, at the tested concentration (data not shown). Next, we evaluated the effect of IFC305 on the expression level of genes associated to the activation process. We found that treatment of HSC with IFC305 at concentrations ranging from 0.2 to 5 mM for 7 days prevented the mRNA expression of collagen α1(I) in a dose-dependent manner, whereas IFC305 at 5 mM stimulated the mRNA expression of MMP-13, PPARγ, and Smad7, three important antifibrogenic genes (Fig. 2A). IFC305 treatment also decreased the protein expression of the HSC activation marker α-SMA and the cell cycle proteins cyclin D1 and cyclin E (Fig. 2B).

Considering that IFC305 is the aspartate salt of adenosine, we also investigated the effect on the cell morphology of HSC cultivated for 7 days in the presence of adenosine or aspartic acid (5 mM). We observed, essentially, the same effect on HSC cultivated with adenosine as that obtained with IFC305 (5 mM), but not with aspartic acid (data not shown). This result suggests

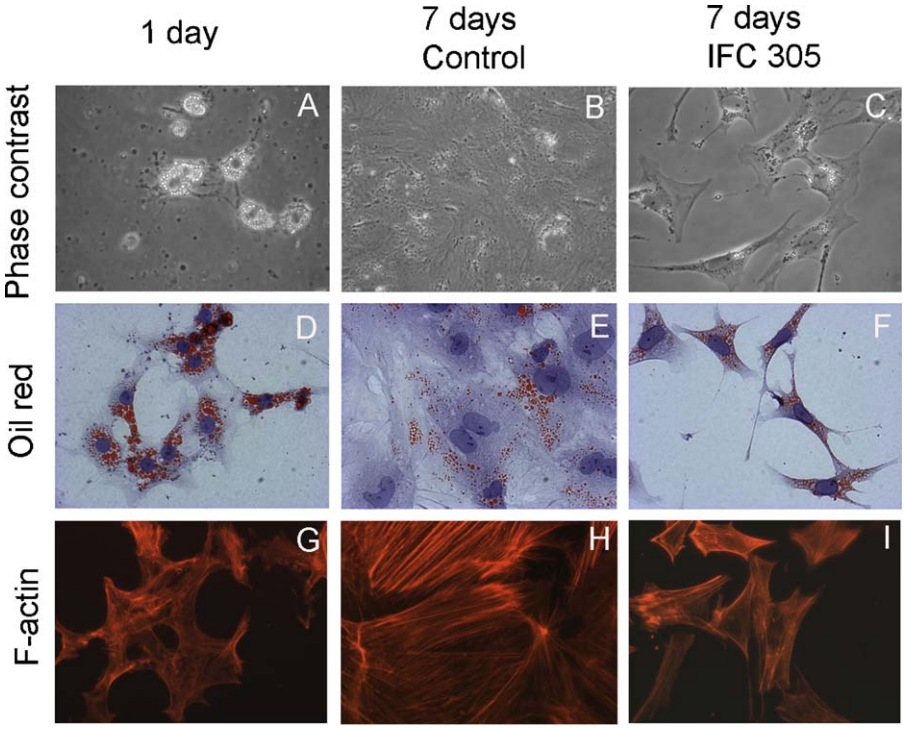

Fig. 1. Morphology of HSC cultivated for 7 days in the presence of IFC305. HSC cultivated for 1 day after isolation from normal rat livers, HSC cultivated for 7 days in absence (Control) or presence of 5 mM IFC305. (A–C) Morphology of HSC observed with a phase-contrast microscopy. (D–F) Oil Red O staining of lipids (red color) and hematoxylin counterstained (blue color). (G–I) F-actin stress fibers stained with Alexa Fluor 532 phalloidin. Magnification, 40×.

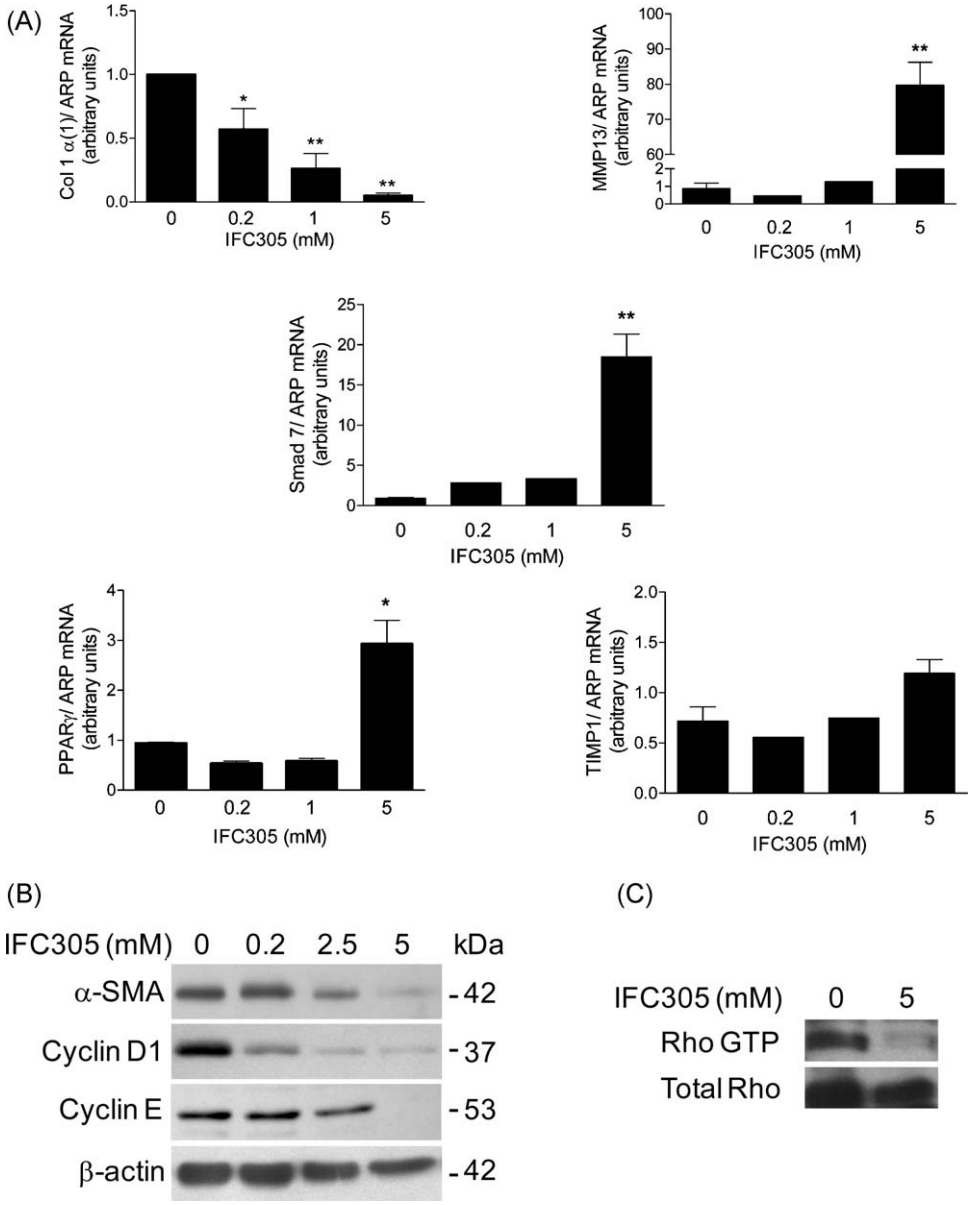

Fig. 2. IFC305 regulates the expression of profibrogenic and antifibrogenic markers in HSC cultivated for 7 days. At 24 h after isolation, cells were incubated with the indicated concentrations of IFC305 for 7 days, changing the medium every other day. (A) Real-time quantitative polymerase chain reaction (qPCR) analysis of the expression of collagen α1(I), MMP-13, Smad7, PPARγ, and TIMP-1 mRNA. Data were normalized to the acidic ribosomal protein (ARP) mRNA expression and are expressed as mean values ± SEM of three independent experiments. $^{*}P < 0.05$ and $^{**}P < 0.01$ versus cells with no IFC305 addition. (B) Western blot analysis of the expression of α-SMA, cyclin D1, and cyclin E proteins. (C) Rho pull-down assay showing activated Rho (Rho-GTP) of HSC cultivated for 7 days without or with 5 mM IFC305. An aliquot from each extract without agarose beads was also analyzed and corresponds to total Rho.

that the adenosine part of IFC305 might exert a greater effect in modifying cellular morphology.

3.2. IFC305 blocks the activation of the Rho/ROCK intracellular signaling pathway

Several research groups have demonstrated that the Rho/ROCK signaling pathway plays an important role in the activation and contraction of HSC [17,18]. HSC activation is accompanied by the formation of actin stress fibers and focal adhesions. Rho has been implicated in the morphological changes associated with HSC activation by regulating the actin cytoskeleton [19]. Recently it has been demonstrated that adenosine induces loss of actin stress fibers and inhibits cellular contraction in activated HSC via Rho/ROCK inhibition [20]. We observed that, as adenosine, IFC305 treatment reduced F-actin stress fibers (Fig. 1H versus I). We therefore explored the effect of IFC305 on the formation of the Rho active GTP-bound complex. Spontaneously activated HSC cultivated for 7 days had a remarkable level of activated Rho; in contrast, HSC treated for 7 days with IFC305 had an almost completely reduced activation of Rho (Fig. 2C). This result shows that IFC305, like adenosine, avoids Rho activation and this effect might be associated to the prevention of HSC activation and reduction of actin stress fibers induced by IFC305.

3.3. IFC305 inhibits PDGF-BB-stimulated proliferation of HSC

Activated HSC become highly proliferative and PDGF is the most potent mitogenic cytokine described for these cells [21]. We evaluated the effect of IFC305 on HSC proliferation stimulated by PDGF, measured by BrdU incorporation. Following isolation, HSC were synchronized by serum starvation for 24 h, and then cell

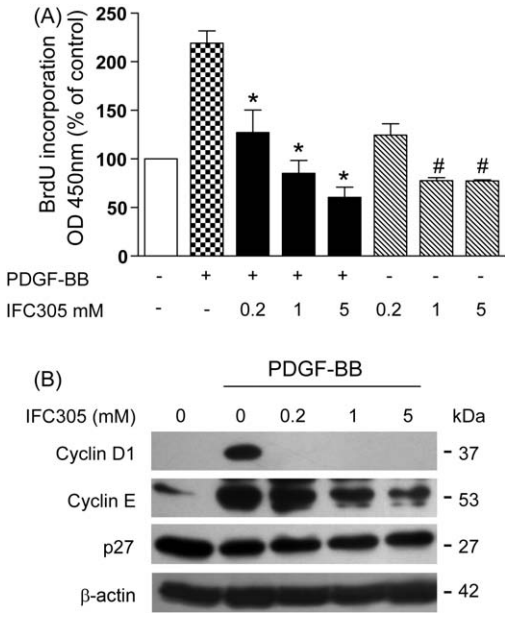

Fig. 3. IFC305 suppresses the PDGF-BB-stimulated proliferation of HSC. (A) Fresh HSC were incubated overnight with DMEM-10% FBS and then serum starved for 24 h. After cellular synchronization, the cells were stimulated in the absence or presence of PDGF-BB (20 ng/ml) and the indicated concentrations of IFC305 for 24 h. Cell proliferation was assessed by BrdU incorporation. Results are expressed as percentage of control (untreated cells). Data are shown as mean ± SEM of three independent experiments. $^{*}P < 0.05$ versus cells stimulated with PDGF-BB and $\#P < 0.05$ versus control cells. (B) Western blot analysis of different cell cycle proteins. Cells were treated as in (A), but with 10 ng/ml of PDGF-BB. Total cell lysate proteins were analyzed by Western blotting as described under Section 2.

proliferation was stimulated with PDGF-BB during 24 h in the presence of different concentrations of IFC305. We found that IFC305 dose-dependently reduced the PDGF-BB-stimulated proliferation (Fig. 3A). Western blot analysis further revealed that IFC305 reduced the expression of different cell cycle proteins stimulated by PDGF-BB, with a marked reduction of cyclin D1, and a lower effect on cyclin E. No changes were seen in the expression of the cell cycle inhibitor protein $p27^{(kip1)}$ with PDGF-BB or with the different concentrations of IFC305 (Fig. 3B). Together these data demonstrate that IFC305 inhibits HSC proliferation stimulated by PDGF-BB.

We also compared the effect of adenosine or aspartic acid with that of IFC305 on the PDGF-BB stimulated proliferation of HSC. We observed that both, adenosine (1 mM) and IFC305 (1 mM) inhibited PDGF-BB-stimulated proliferation of HSC in a similar manner (82.5 ± 2.6% and 76.5 ± 3.3%, respectively). In contrast, aspartic acid (1 mM) only reduced 27.7 ± 4.3% PDGF-BB-induced proliferation. As in the previous observation on the cell morphology of HSC with adenosine, this result suggests that the adenosine part of IFC305 might have the principal effect on the inhibition of HSC proliferation.

3.4. IFC305 modulates the intracellular signaling pathways activated by PDGF-BB

To explore further the molecular mechanism mediating the inhibitory effect of IFC305 on PDGF-induced proliferation of HSC, we examined the most important pathways stimulated by PDGF-BB in HSC [22–25]. Increased phosphorylation of ERK, AKT, p70S6K, and p-JNK was observed after 30 min of PDGF-BB stimulation; at this early time point, IFC305 did not modify the activation of Erk and AKT, it only slightly inhibited the activation of p70S6K and markedly reduced the 54 kDa form of p-JNK (Fig. 4). However, when stimulation with PDGF-BB was continued for 24 h, treatment of HSC with IFC305 effectively inhibited PDGF-induced phospho-

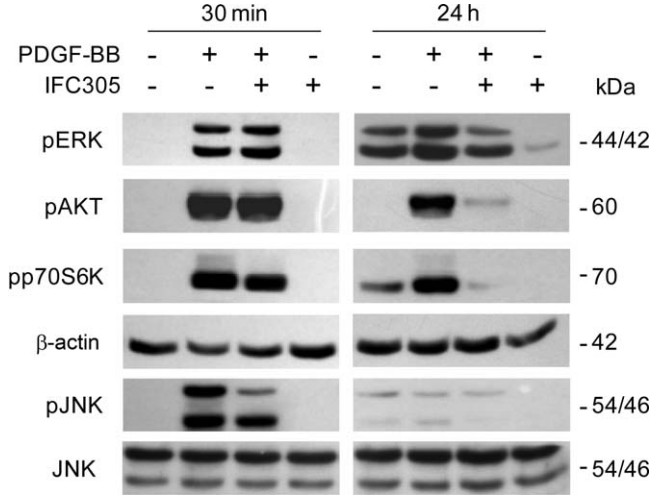

Fig. 4. IFC305 modulates the signaling pathways stimulated by PDGF-BB. Fresh HSC were incubated overnight with DMEM-10% FBS and serum starved for 24 h. Then, the cells were stimulated with PDGF-BB (10 ng/ml) and/or IFC305 (5 mM) for 30 min or 24 h. Cells were lysed and analyzed by Western blotting with the indicated antibodies.

AKT and p70S6K levels, and partially suppressed phosphorylation of ERK (Fig. 4). At 24 h, we also observed an increment of the basal phosphorylation of ERK and p70S6K, larger than the basal phospho-levels at 30 min, probably due to the extended period without serum (48 h). These results indicate that IFC305 does not affect the early activation of ERK, p70S6K, and AKT pathway induced by PDGF-BB, but inhibits the late stimulation at 24 h.

3.5. Adenosine receptors are not involved in HSC growth inhibition by IFC305

Extracellular adenosine can exert its actions on cells either by adenosine receptors or by entering the cells by adenosine transporters [26,27]. To characterize the molecular mechanism by which IFC305 inhibited HSC proliferation, we first addressed the question whether this compound could be interacting with adenosine receptors. We explored the possibility that IFC305 might inhibit HSC proliferation by a specific subtype of the four known adenosine receptors; A_1, A_{2A}, A_{2B} and A_3 [3]. HSC were pretreated for 30 min before the proliferation assay by BrdU incorporation with different adenosine receptor antagonists. As shown in Fig. 5A–E none of the antagonists used alone or in combination prevented the IFC305-induced inhibition of proliferation. These results indicate that IFC305 effects are not mediated via adenosine receptors activation, probably exerting its action by an intracellular mechanism.

3.6. Involvement of adenosine kinase in IFC305-induced cell growth inhibition

To determine if IFC305 might be entering the cell through adenosine transporters to exert its anti-proliferative action, we examined the effect of NBTI and dipyridamole, two inhibitors of these transporters. We observed that both compounds significantly reversed the IFC305-mediated growth inhibition (Fig. 6A and B), suggesting that the uptake of IFC305 by an adenosine transporter is involved in the inhibition of proliferation exerted by IFC305. Intracellular adenosine can be metabolized by adenosine deaminase, which converts adenosine to inosine, or by adenosine kinase, which catalyzes the formation of AMP from adenosine through its phosphorylation. The action of IFC305 was not affected by EHNA, an adenosine deaminase inhibitor (Fig. 6C), but it was significantly

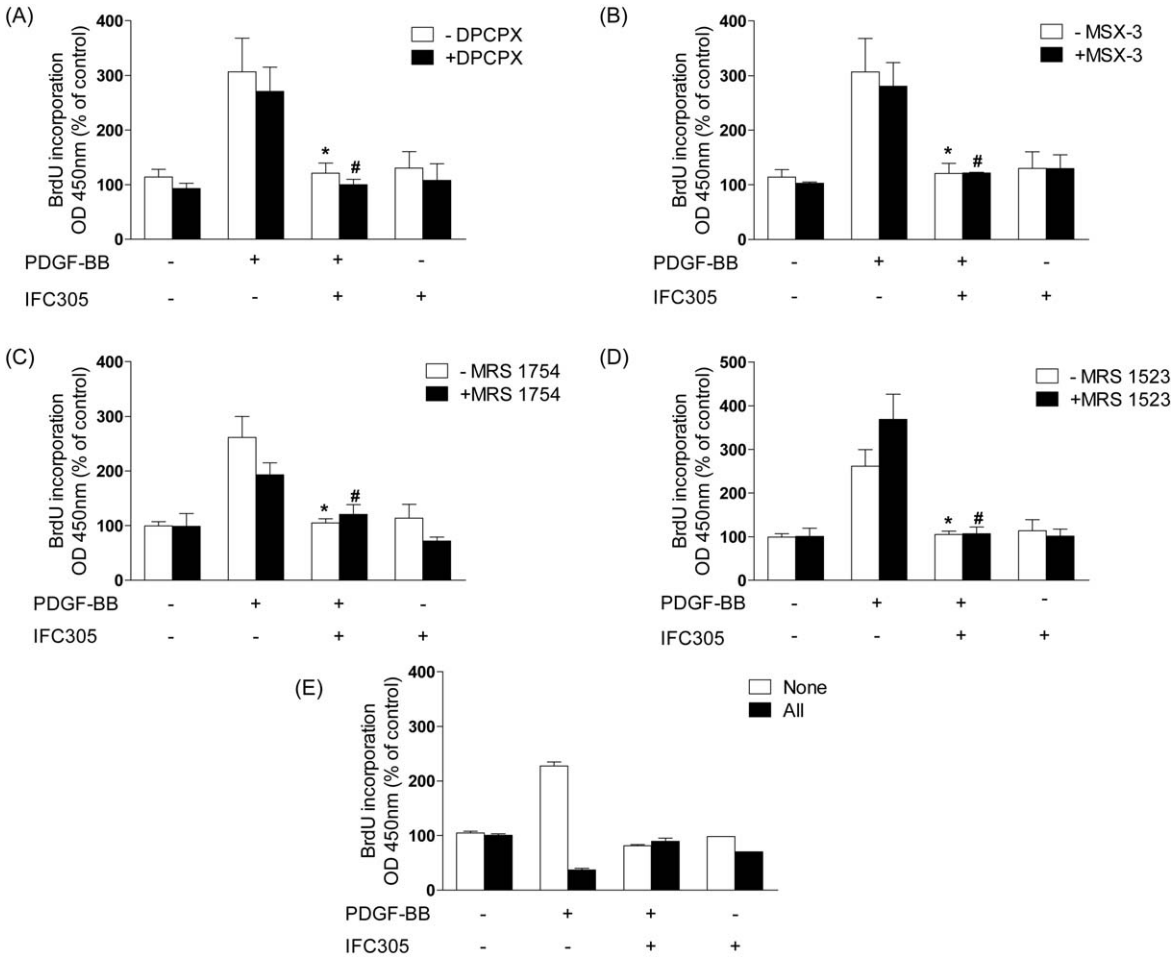

Fig. 5. Adenosine receptors are not involved in the IFC305-inhibition of the PDGF-BB-stimulated proliferation of HSC. BrdU incorporation assay was performed as in Fig. 3, but the cells were pre-incubated in the presence of vehicles (open bars) or the indicated adenosine receptor antagonists (solid bars) for 30 min before the addition of 20 ng/ml PDGF-BB and 1 mM IFC305. The following adenosine receptor antagonists were used: (A) DPCPX, A_1 receptor antagonist (100 nM). (B) MSX-3, A_{2A} receptor antagonist (10 μM). (C) MRS 1754, A_{2B} receptor antagonist (10 μM). (D) MRS 1523, A_3 receptor antagonist (10 μM). (E) Combination of the four antagonists. Results are expressed as percentage of control (untreated cells with vehicle). Data are shown as mean ± SEM of three independent experiments. $^*P < 0.05$ versus PDGF-BB-treated cells with vehicle, $\#P < 0.05$ versus PDGF-BB-treated cells with antagonist.

inhibited by AMDA, an adenosine kinase inhibitor (Fig. 6D), suggesting that IFC305 transported from the extracellular space may inhibit HSC proliferation through its conversion to AMP by adenosine kinase. Intracellular AMP could stimulate AMP-activated protein kinase (AMPK) by promoting its phosphorylation at the threonine (Thr-172) on the alpha-subunit [4,28]. In order to test if IFC305 could be inhibiting HSC proliferation via activation of AMPK, we tried to detect an increased phosphorylation of Thr-172 with IFC305 treatment. As shown in Fig. 7, rather than increasing phospho-AMPK levels, IFC305 inhibited both, basal and PDGF-stimulated phosphorylation of AMPK. These results suggest that AMPK activation would not be involved in the IFC305-mediated inhibition of proliferation, although AMP formation inside the cell is necessary for growth inhibition.

3.7. Uridine reverses the inhibitory effect of IFC305 on HSC proliferation and activation

Several studies have demonstrated that extracellular adenosine may cause intracellular pyrimidine starvation, thereby blocking DNA synthesis and inhibiting cell growth. Accumulation of intracellular AMP increases intracellular ATP and ADP levels but reduces pyrimidine nucleotides, such as UTP, and this effect is reversed when uridine is added to the extracellular space [5–7,29]. We therefore added uridine at different concentrations and observed that IFC305-induced cell growth inhibition was reversed (Fig. 8A), suggesting that intracellular pyrimidine starvation could be involved in the IFC305-inhibition of proliferation. We further investigated whether uridine would be involved not only in the suppressive effect of IFC305 on HSC proliferation, but also in the inhibitory effect of IFC305 on the HSC activation process. When uridine was included in the medium of HSC cultivated with IFC305 for 7 days, the cells became activated as demonstrated by their loss of stellate morphology characteristic of quiescent HSC and expression of α-SMA (Fig. 8B and C). We also determined levels of intracellular AMP by HPLC in HSC cultivated for 7 days in the absence or presence of IFC305 or IFC305 plus uridine, and we observed that in both cases AMP content was incremented at least 4-fold over the control (data not shown). Therefore, uridine addition does not block the elevation of intracellular AMP levels induced by IFC305, but instead it seems to regenerate the pyrimidine nucleotide pool via the pyrimidine salvage pathway [7] that may compensate the balance of nucleotide pools restoring DNA synthesis and HSC proliferation. Collectively these results suggest that extracellular IFC305 is incorporated into HSC by adenosine transporters where it is converted to AMP by adenosine kinase, and the increased AMP level may inhibit HSC cell growth and activation through the unbalanced nucleotide pool.

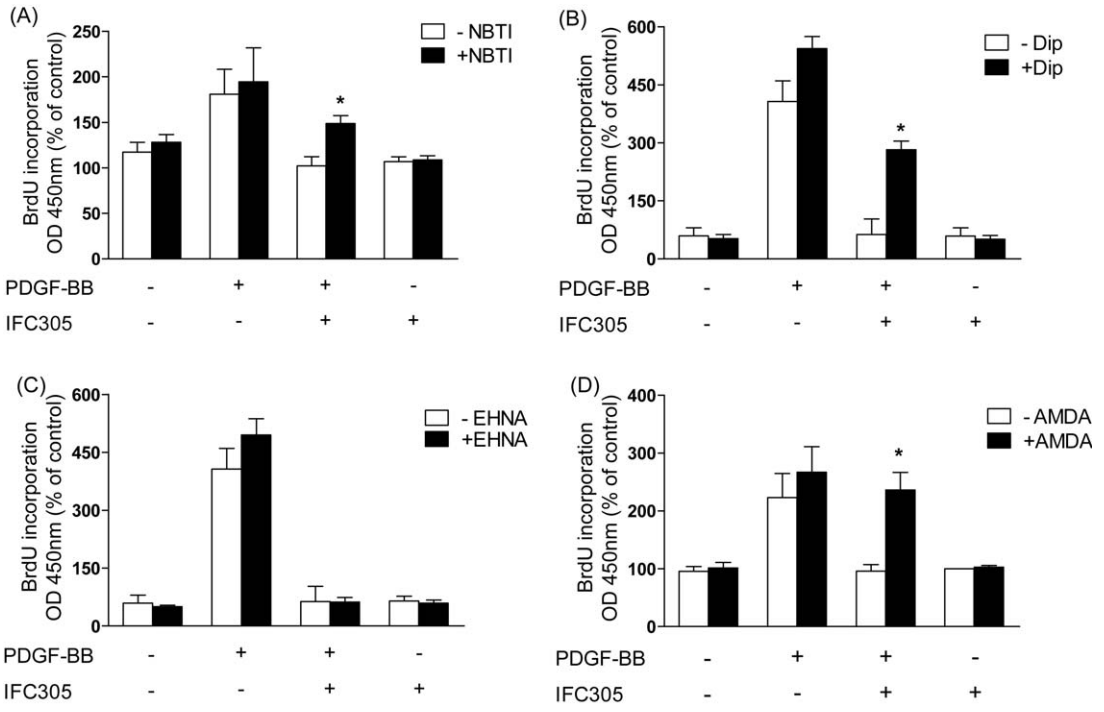

Fig. 6. AMDA inhibition of adenosine kinase suppresses the IFC305-inhibition of the PDGF-BB-stimulated proliferation of HSC. BrdU incorporation assay was performed as in Fig. 3, but the cells were pre-incubated in the presence of vehicles (open bars) or the indicated inhibitors (solid bars) for 30 min before the addition of 20 ng/ml PDGF-BB and 1 mM IFC305. The following inhibitors were used: (A) NBTI, equilibrative adenosine transporters inhibitor (10 μM). (B) Dip, dipyridamole, equilibrative adenosine transporters inhibitor (10 μM). (C) EHNA, adenosine deaminase inhibitor (10 μM). (D) AMDA, adenosine kinase inhibitor (10 μM). Results are expressed as percentage of control (untreated cells with vehicle). Data are shown as mean ± SEM of three independent experiments. $^{*}P < 0.05$ versus PDGF-BB/IFC305 treated cells with vehicle.

4. Discussion

In a previous study we demonstrated that the adenosine aspartate compound IFC305 reversed established liver fibrosis in rats [14]. To further characterize the molecular and cellular mechanisms responsible for this reversing capacity, the present study explored the effect of IFC305 on the activation of primary rat HSC cultivated *in vitro*. We found that IFC305 treatment suppresses HSC activation, as assessed by the inhibition of α-SMA protein and collagen α1(I) mRNA expression, prevention of Rho activation, suppression of PDGF-stimulated proliferation and increased expression of antifibrogenic genes such as PPARγ, Smad7, and MMP-13.

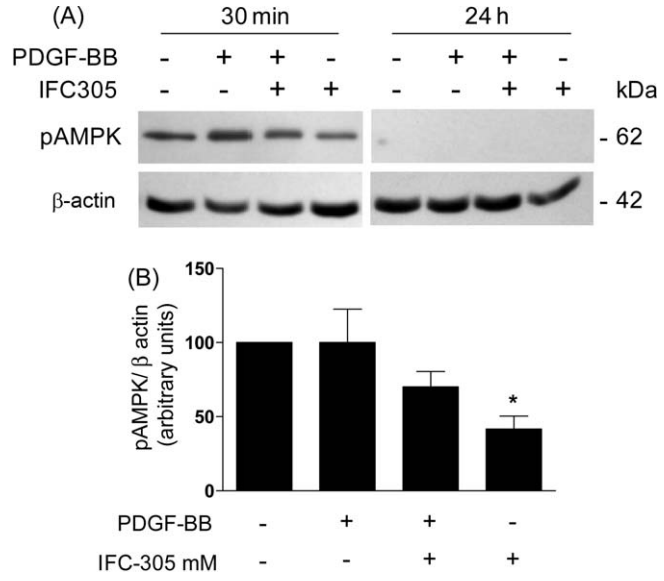

Fig. 7. Role of IFC305 on the phosphorylation of AMPK induced by PDGF. (A) Fresh HSC were incubated overnight with DMEM-10% FBS and serum starved for 24 h, then stimulated with 10 ng/ml PDGF-BB in the absence or presence of 5 mM IFC305 for 30 min or 24 h. Cells were lysed and analyzed by Western blotting with the indicated antibodies. (B) Quantification of pAMPK bands normalized with β-actin of cells treated for 30 min. Data are shown as mean ± SEM of three independent experiments. $^{*}P < 0.01$ versus control cells.

Hepatic fibrosis is characterized by ECM components accumulation, mainly type I collagen. The excess of ECM components is the result of an imbalance between their production and degradation. ECM degradation is done by matrix metalloproteinases (MMPs), whose activity is negatively regulated by tissue inhibitors of matrix metalloproteinases (TIMPs). During progression of liver fibrosis, activated HSC produce an excess of type I collagen and have a sustained production of TIMP-1 and -2, resulting in an excess of collagen deposition. The main MMPs that can degrade native type I collagen in humans are MMP-1 and -8 (MMP-13 is the rodent equivalent of human MMP-1). In this study we demonstrate that IFC305 is able to inhibit the production of collagen α1(I) mRNA, and to increase the expression of MMP-13 mRNA, which may result in an important decrease of collagen deposition, even though the expression of TIMP-1 was not altered by the IFC305 treatment. Our results are in agreement with a study that suggests that type I collagen and MMP-13 mRNAs are reciprocally modulated in HSC, when type I collagen expression is increased, MMP-13 expression is diminished [30]. TGF-β is one of the most important fibrogenic cytokines in different tissues, including liver, lung, and kidney. Disruption of TGF-β signaling pathway has been suggested as an important antifibrotic therapy [31]. TGF-β signals through the Type I, II, and III (betaglycan) membrane receptors and by intracellular Smad proteins, mainly Smad2, 3, 4, and 7. Smad7 is the most important endogenous intracellular antagonist of TGF-β signaling and its over-expression has been used to prevent HSC activation *in vivo* and *in vitro* [32,33]. Increased expression of

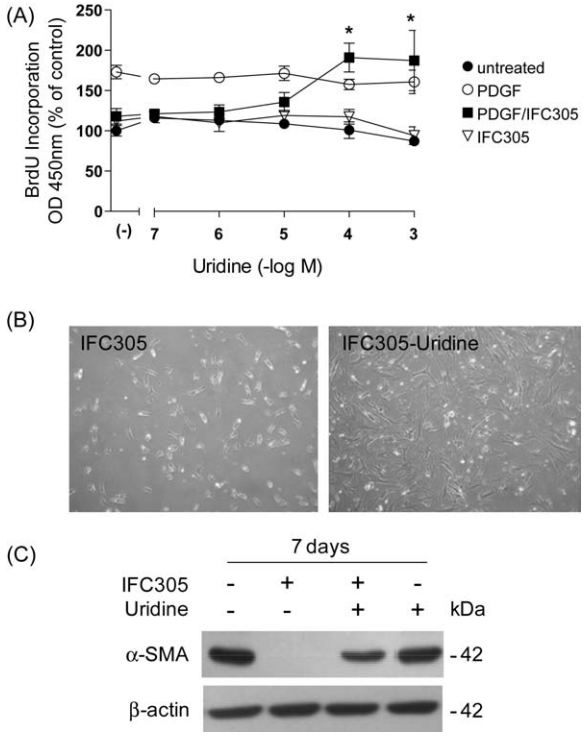

Fig. 8. Uridine reverses the inhibitory effect of IFC305 on HSC proliferation and activation. (A) BrdU incorporation assay was performed as in Fig. 3, but the cells were pre-incubated with various concentrations of uridine for 15 min before the addition of 20 ng/ml PDGF-BB and 1 mM IFC305. Results are expressed as percentage of control (untreated cells without uridine). Data are shown as mean ± SEM of three independent experiments. *$P < 0.05$ versus PDGF/IFC305 treated cells without uridine (−). (B) HSC cultivated for 7 days with IFC305 (5 mM) alone or in the presence of uridine (1 mM), cell morphology observed with a phase-contrast microscopy. Magnification, 10×. (C) Western blot analysis of α-SMA protein expression of HSC cultivated for 7 days with IFC305 (5 mM) and uridine (1 mM) as indicated.

Smad7 induced by IFC305 treatment could result in the inhibition of TGF-β signaling and inhibition of HSC activation. Another main effect of IFC305 on HSC is an increase of PPARγ expression. PPARγ is a ligand-dependent transcription factor that regulates adipocyte differentiation and lipid metabolism. PPARγ is highly expressed in quiescent HSC, but its expression is rapidly decreased during HSC activation *in vitro* and *in vivo* [34]. Forced expression of PPARγ can reverse the activated HSC phenotype to the quiescent one [35], and treatment of activated HSC with natural or synthetic ligands of PPARγ inhibits their activation [34,36]. Indeed, the PPARγ ligands 15-deoxy-prostaglandin J2 (15d-PGJ2) and ciglitizone are considered antifibrotic, and they have been proposed as therapy for chronic liver diseases [37,38]. Thus, the increased expression of PPARγ by HSC with IFC305 treatment could be contributing to maintain their quiescent phenotype. One possible mechanism by which IFC305 could be altering the transcription of these genes is by modifying the metabolism of S-adenosyl methionine (SAMe) involved in epigenetic changes such as DNA methylation. We have previously demonstrated that there is a close relationship between adenosine's level, SAMe and transmethylation reactions in the liver [39]. However a possible epigenetic modulation by IFC305 similar to that of adenosine is being studied.

The Rho/ROCK signaling pathway has been implicated in the activation of HSC. Several studies have determined that inhibition of Rho signaling could prevent HSC activation [17,18,40]. Our result demonstrates that HSC treated for 7 days with IFC305 have an almost completely abated Rho activation, and this effect could be contributing to maintain their quiescent state. IFC305 seems to have a similar effect as that of adenosine because our result coincides with a study demonstrating that adenosine inhibits the Rho/ROCK signaling in activated HSC [20]. However, our results differ from previous findings in which this research group reported that adenosine stimulates collagen expression [41]. This could be associated to differences in the cellular model, instead of primary cultured HSC, these studies were mainly done with LX-2 cells, an immortalized human HSC line, using a low concentration of adenosine (10 μM) and different A_{2A} receptor agonists, such as CGS21680 and NECA [41,42].

Another remarkable feature of HSC activation is their increased proliferation, involved in sustaining liver fibrosis. PDGF is the most potent growth factor for HSC and this cytokine and its receptor are up-regulated as they become activated [23,43,44]. We found that IFC305 inhibits PDGF-stimulated proliferation (Fig. 3A), and although IFC305 has no effect on the PDGF-induced phosphorylation of Erk, AKT, and p70S6K at 30 min, when stimulation is continued for 24 h, IFC305 inhibited their phosphorylation (Fig. 4); at these late time points, activation of ERK and AKT is related to cell cycle progression [45,46]. The sustained activation of ERK1 is required for the continued expression of cyclin D1 in G1 cell cycle progression [45]. We also observed a drastic reduction in cyclin D1 protein expression in HSC treated with IFC305 (Figs. 2 and 3). On the other hand, a late peak of ERK and AKT activation is necessary for G2/M phase [46]. These results indicate that IFC305 does not interfere with the early activation pathways stimulated by PDGF, but inhibits the late ones, necessary for cell cycle progression.

Our data showed that inhibition of PDGF-induced proliferation by IFC305 is not mediated by adenosine receptors, since none of the specific antagonists of each receptor type blocked the effect of IFC305 (Fig. 5A–E). In contrast, the inhibition of adenosine transporters by NBT1 and dipyridamole, as well as the inhibition of adenosine kinase by AMDA, suggests that IFC305 inhibits PDGF-induced proliferation by its uptake into cells through adenosine transporters and its conversion to AMP by adenosine kinase, leading to an increase in intracellular AMP levels (Fig. 6A, B and D). Intracellular elevation of the AMP/ATP ratio could stimulate activation of AMP-activated protein kinase (AMPK) by promoting its phosphorylation at threonine (Thr-172) on the alpha-subunit [4,28]. Recently, it has been reported that AMPK activation by adiponectin, AICAR, or metformin inhibits proliferation of activated HSC and negatively modulates their activated phenotype [47,48]. We therefore tried to detect an increased phosphorylation of AMPK with IFC305. We observed that phospho-AMPK level was slightly increased with PDGF, but this was not incremented with IFC305 treatment, and the basal phosphorylation of AMPK was even reduced with IFC305 (Fig. 7). These results suggest that AMPK activation would not be involved in IFC305-mediated inhibition of proliferation.

Another mechanism that has been proposed for the growth inhibition by extracellular adenosine is by reducing pyrimidine nucleotides through a mechanism known as "pyrimidine starvation". Accumulation of AMP generated by adenosine kinase action can lead to inhibition of 5-phosphoribosyl-1-pyrophosphate (PRPP) synthase [49,50]. This will lead to a decreased PRPP level, an essential component in the purine and pyrimidine "*de novo*" biosynthesis that finally will result in decreased UTP and CTP levels [5]. Pyrimidine starvation can be relieved by addition of uridine that is converted to UMP, which is used to synthetisize pyrimidine nucleotides via the pyrimidine salvage pathway [7]. We showed that uridine not only reversed the proliferative inhibition of HSC by IFC305, but also reversed the inhibitory effect of this compound on the activation process (Fig. 8), suggesting the importance of pyrimidine starvation in cellular differentiation [51]. Thus, our results suggest that the anti-proliferative effect of IFC305 requires its uptake into cells by adenosine transporters followed by its

intracellular conversion to AMP by adenosine kinase, leading to increased levels of AMP, pyrimidine starvation, and inhibition of DNA synthesis.

In conclusion, the present study demonstrates that the adenosine aspartate compound, IFC305, suppresses the activation of primary cultured HSC. IFC305 seems to maintain the quiescent state of HSC maintaining PPARγ expression and inhibiting Rho activation, which is reflected on the decreased expression of the characteristic features of activated HSC, such as collagen α1(I) and α-SMA. We also demonstrate that IFC305 inhibits PDGF-BB-stimulated proliferation, a fundamental feature of HSC activation, possibly through increased AMP levels and pyrimidine starvation. This effect of IFC305 on nucleotides metabolism probably impairs DNA synthesis and cell proliferation. On the other hand, IFC305 increases the expression of two critical antifibrogenic genes such as Smad7 and MMP-13. Some of these findings are similar to the actions of IFC305 observed in our previous *in vivo* experiment regarding HSC. In that study, we observed that in the liver of CCl_4-induced cirrhotic rats, IFC305 treatment reduced the number of α-SMA activated HSC, increased the amount of lipid-storing HSC, and up-regulated the gene expression of PPARγ [14]. We are aware that some of the *in vitro* effects of IFC305 were observed at higher concentrations than those that may be reached *in vivo*; nevertheless, we observed that this compound had no toxic effects on cultured HSC and such concentrations have been used for adenosine in other *in vitro* studies [52,53]. Thus, our study proposes that HSC are an important target of the antifibrotic action of IFC305, but it might be possible that the beneficial effect *in vivo* could be more complex and involve other hepatic cells. This study, together with our previous observations on the protective effect of IFC305 on liver fibrosis, suggests that this compound might offer therapeutic potential through a variety of biochemical mechanisms.

Acknowledgements

We greatly appreciate Minerva Mora's technical assistance from our institutional Molecular Biology core facility and Rosario Villaseñor for valuable secretarial assistance. This work was supported by, the Consejo Nacional de Ciencia y Tecnología CONACYT 82298.

References

[1] Friedman SL. Hepatic stellate cells: protean, multifunctional, and enigmatic cells of the liver. Physiol Rev 2008;88:125–72.
[2] Zimmermann H. Extracellular metabolism of ATP and other nucleotides. Naunyn Schmiedebergs Arch Pharmacol 2000;362:299–309.
[3] Fredholm BB. Adenosine, an endogenous distress signal, modulates tissue damage and repair. Cell Death Differ 2007;14:1315–23.
[4] Hardie DG. AMPK: a key regulator of energy balance in the single cell and the whole organism. Int J Obes (Lond) 2008;32(Suppl. 4):S7–12.
[5] Snyder FF, Seegmiller JE. The adenosine-like effect of exogenous cyclic AMP upon nucleotide and PP-ribose-P concentrations of cultured human lymphoblasts. FEBS Lett 1976;66:102–6.
[6] Weisman GA, Lustig KD, Lane E, Huang NN, Belzer I, Friedberg I. Growth inhibition of transformed mouse fibroblasts by adenine nucleotides occurs via generation of extracellular adenosine. J Biol Chem 1988;263:12367–72.
[7] Seetulsingh-Goorah SP. Mechanisms of adenosine-induced cytotoxicity and their clinical and physiological implications. Biofactors 2006;27:213–30.
[8] Hernandez-Munoz R, Glender W, Diaz-Munoz M, Adolfo J, Garcia-Sainz JA, Chagoya de Sanchez V. Effects of adenosine on liver cell damage induced by carbon tetrachloride. Biochem Pharmacol 1984;33:2599–604.
[9] Hernandez-Munoz R, Diaz-Munoz M, Suarez J, Chagoya de Sanchez V. Adenosine partially prevents cirrhosis induced by carbon tetrachloride in rats. Hepatology 1990;12:242–8.
[10] Hernandez-Munoz R, Diaz-Munoz M, Chagoya de Sanchez V. Effects of adenosine administration on the function and membrane composition of liver mitochondria in carbon tetrachloride-induced cirrhosis. Arch Biochem Biophys 1992;294:160–7.
[11] Hernandez-Munoz R, Diaz-Munoz M, Chagoya de Sanchez V. Possible role of cell redox state on collagen metabolism in carbon tetrachloride-induced cirrhosis as evidenced by adenosine administration to rats. Biochim Biophys Acta 1994;1200:93–9.
[12] Chagoya de Sanchez V, Hernandez-Munoz R, Yanez L, Vidrio S, Diaz-Munoz M. Possible mechanism of adenosine protection in carbon tetrachloride acute hepatotoxicity. Role of adenosine by-products and glutathione peroxidase. J Biochem Toxicol 1995;10:41–50.
[13] Hernandez-Munoz R, Diaz-Munoz M, Suarez-Cuenca JA, Trejo-Solis C, Lopez V, Sanchez-Sevilla L, et al. Adenosine reverses a preestablished CCl4-induced micronodular cirrhosis through enhancing collagenolytic activity and stimulating hepatocyte cell proliferation in rats. Hepatology 2001;34:677–87.
[14] Perez-Carreon JI, Martinez-Perez L, Loredo ML, Yanez-Maldonado L, Velasco-Loyden G, Vidrio-Gomez S, et al. An adenosine derivative compound, IFC305, reverses fibrosis and alters gene expression in a pre-established CCl(4)-induced rat cirrhosis. Int J Biochem Cell Biol 2010;42:287–96.
[15] Yassuda Filho P, Bracht A, Ishii-Iwamoto EL, Lousano SH, Bracht L, Kelmer-Bracht AM. The urea cycle in the liver of arthritic rats. Mol Cell Biochem 2003;243:97–106.
[16] Schafer S, Zerbe O, Gressner AM. The synthesis of proteoglycans in fat-storing cells of rat liver. Hepatology 1987;7:680–7.
[17] Murata T, Arii S, Nakamura T, Mori A, Kaido T, Furuyama H, et al. Inhibitory effect of Y-27632, a ROCK inhibitor, on progression of rat liver fibrosis in association with inactivation of hepatic stellate cells. J Hepatol 2001;35:474–81.
[18] Higashi N, Kohjima M, Fukushima M, Ohta S, Kotoh K, Enjoji M, et al. Epigallocatechin-3-gallate, a green-tea polyphenol, suppresses Rho signaling in TWNT-4 human hepatic stellate cells. J Lab Clin Med 2005;145:316–22.
[19] Yee Jr HF. Rho directs activation-associated changes in rat hepatic stellate cell morphology via regulation of the actin cytoskeleton. Hepatology 1998;28:843–50.
[20] Sohail MA, Hashmi AZ, Hakim W, Watanabe A, Zipprich A, Groszmann RJ, et al. Adenosine induces loss of actin stress fibers and inhibits contraction in hepatic stellate cells via Rho inhibition. Hepatology 2009;49:185–94.
[21] Pinzani M, Gesualdo L, Sabbah GM, Abboud HE. Effects of platelet-derived growth factor and other polypeptide mitogens on DNA synthesis and growth of cultured rat liver fat-storing cells. J Clin Invest 1989;84:1786–93.
[22] Marra F, Gentilini A, Pinzani M, Choudhury GG, Parola M, Herbst H, et al. Phosphatidylinositol 3-kinase is required for platelet-derived growth factor's actions on hepatic stellate cells. Gastroenterology 1997;112:1297–306.
[23] Pinzani M. PDGF and signal transduction in hepatic stellate cells. Front Biosci 2002;7:d1720–6.
[24] Gabele E, Reif S, Tsukada S, Bataller R, Yata Y, Morris T, et al. The role of p70S6K in hepatic stellate cell collagen gene expression and cell proliferation. J Biol Chem 2005;280:13374–82.
[25] Bridle KR, Li L, O'Neill R, Britton RS, Bacon BR. Coordinate activation of intracellular signaling pathways by insulin-like growth factor-1 and platelet-derived growth factor in rat hepatic stellate cells. J Lab Clin Med 2006;147:234–41.
[26] Pastor-Anglada M, Cano-Soldado P, Errasti-Murugarren E, Casado FJ. SLC28 genes and concentrative nucleoside transporter (CNT) proteins. Xenobiotica 2008;38:972–94.
[27] Molina-Arcas M, Trigueros-Motos L, Casado FJ, Pastor-Anglada M. Physiological and pharmacological roles of nucleoside transporter proteins. Nucleos Nucleot Nucl Acids 2008;27:769–78.
[28] Hardie DG. The AMP-activated protein kinase pathway—new players upstream and downstream. J Cell Sci 2004;117:5479–87.
[29] Ohkubo S, Nagata K, Nakahata N. Adenosine uptake-dependent C6 cell growth inhibition. Eur J Pharmacol 2007;577:35–43.
[30] Schaefer B, Rivas-Estilla AM, Meraz-Cruz N, Reyes-Romero MA, Hernandez-Nazara ZH, Dominguez-Rosales JA, et al. Reciprocal modulation of matrix metalloproteinase-13 and type I collagen genes in rat hepatic stellate cells. Am J Pathol 2003;162:1771–80.
[31] Tsukada S, Parsons CJ, Rippe RA. Mechanisms of liver fibrosis. Clin Chim Acta 2006;364:33–60.
[32] Chen YW, Li DG, Wu JX, Lu HM. Tetrandrine inhibits activation of rat hepatic stellate cells stimulated by transforming growth factor-beta in vitro via up-regulation of Smad 7. J Ethnopharmacol 2005;100:299–305.
[33] Dooley S, Hamzavi J, Breitkopf K, Wiercinska E, Said HM, Lorenzen J, et al. Smad7 prevents activation of hepatic stellate cells and liver fibrosis in rats. Gastroenterology 2003;125:178–91.
[34] Miyahara T, Schrum L, Rippe R, Xiong S, Yee Jr HF, Motomura K, et al. Peroxisome proliferator-activated receptors and hepatic stellate cell activation. J Biol Chem 2000;275:35715–22.
[35] Hazra S, Xiong S, Wang J, Rippe RA, Krishna V, Chatterjee K, et al. Peroxisome proliferator-activated receptor gamma induces a phenotypic switch from activated to quiescent hepatic stellate cells. J Biol Chem 2004;279:11392–401.
[36] Guo YT, Leng XS, Li T, Peng JR, Song SH, Xiong LF, et al. Effect of ligand of peroxisome proliferator-activated receptor gamma on the biological characters of hepatic stellate cells. World J Gastroenterol 2005;11:4735–9.
[37] Neuschwander-Tetri BA, Brunt EM, Wehmeier KR, Oliver D, Bacon BR. Improved nonalcoholic steatohepatitis after 48 weeks of treatment with the PPAR-gamma ligand rosiglitazone. Hepatology 2003;38:1008–17.
[38] Belfort R, Harrison SA, Brown K, Darland C, Finch J, Hardies J, et al. A placebo-controlled trial of pioglitazone in subjects with nonalcoholic steatohepatitis. N Engl J Med 2006;355:2297–307.
[39] Chagoya de Sanchez V, Hernandez-Munoz R, Sanchez L, Vidrio S, Yanez L, Suarez J. Twenty-four-hour changes of S-adenosylmethionine, S-adenosylhomocysteine adenosine and their metabolizing enzymes in rat liver; possible physiological significance in phospholipid methylation. Int J Biochem 1991;23:1439–43.

[40] Tada S, Iwamoto H, Nakamuta M, Sugimoto R, Enjoji M, Nakashima Y, et al. A selective ROCK inhibitor, Y27632, prevents dimethylnitrosamine-induced hepatic fibrosis in rats. J Hepatol 2001;34:529–36.
[41] Hashmi AZ, Hakim W, Kruglov EA, Watanabe A, Watkins W, Dranoff JA, et al. Adenosine inhibits cytosolic calcium signals and chemotaxis in hepatic stellate cells. Am J Physiol Gastrointest Liver Physiol 2007;292:G395–401.
[42] Che J, Chan ES, Cronstein BN. Adenosine A2A receptor occupancy stimulates collagen expression by hepatic stellate cells via pathways involving protein kinase A, Src, and extracellular signal-regulated kinases 1/2 signaling cascade or p38 mitogen-activated protein kinase signaling pathway. Mol Pharmacol 2007;72:1626–36.
[43] Pinzani M, Marra F, Carloni V. Signal transduction in hepatic stellate cells. Liver 1998;18:2–13.
[44] Wong L, Yamasaki G, Johnson RJ, Friedman SL. Induction of beta-platelet-derived growth factor receptor in rat hepatic lipocytes during cellular activation in vivo and in culture. J Clin Invest 1994;94:1563–9.
[45] Weber JD, Raben DM, Phillips PJ, Baldassare JJ. Sustained activation of extracellular-signal-regulated kinase 1 (ERK1) is required for the continued expression of cyclin D1 in G1 phase. Biochem J 1997;326(Pt 1):61–8.
[46] Roberts EC, Shapiro PS, Nahreini TS, Pages G, Pouyssegur J, Ahn NG. Distinct cell cycle timing requirements for extracellular signal-regulated kinase and phosphoinositide 3-kinase signaling pathways in somatic cell mitosis. Mol Cell Biol 2002;22:7226–41.
[47] Adachi M, Brenner DA. High molecular weight adiponectin inhibits proliferation of hepatic stellate cells via activation of adenosine monophosphate-activated protein kinase. Hepatology 2008;47:677–85.
[48] Caligiuri A, Bertolani C, Guerra CT, Aleffi S, Galastri S, Trappoliere M, et al. Adenosine monophosphate-activated protein kinase modulates the activated phenotype of hepatic stellate cells. Hepatology 2008;47:668–76.
[49] Danks MK, Scholar EM. Regulation of phosphoribosylpyrophosphate synthetase by endogenous purine and pyrimidine compounds and synthetic analogs in normal and leukemic white blood cells. Biochem Pharmacol 1982;31:1687–91.
[50] van der Kraan PM, van Zandvoort PM, De Abreu RA, van Baal JM, Bakkeren JA. Inhibition of lymphoid cell growth by adenine ribonucleotide accumulation. The role of phosphoribosylpyrophosphate-depletion induced pyrimidine starvation. Biochim Biophys Acta 1987;927:213–21.
[51] Huang M, Graves LM. De novo synthesis of pyrimidine nucleotides; emerging interfaces with signal transduction pathways. Cell Mol Life Sci 2003;60:321–36.
[52] Yang D, Yaguchi T, Yamamoto H, Nishizaki T. Intracellularly transported adenosine induces apoptosis in HuH-7 human hepatoma cells by downregulating c-FLIP expression causing caspase-3/-8 activation. Biochem Pharmacol 2007;73:1665–75.
[53] Saitoh M, Nagai K, Nakagawa K, Yamamura T, Yamamoto S, Nishizaki T. Adenosine induces apoptosis in the human gastric cancer cells via an intrinsic pathway relevant to activation of AMP-activated protein kinase. Biochem Pharmacol 2004;67:2005–11.